

1 Geochronological constraint on the Cambrian Chengjiang biota,  
2 South China

3  
4  
5 Chuan Yang<sup>1</sup>, Xian-Hua Li<sup>1,3,\*</sup>, Maoyan Zhu<sup>2,3</sup>, Daniel J. Condon<sup>4</sup> & Junyuan Chen<sup>2,5</sup>  
6  
7

8 1 State Key Laboratory of Lithospheric Evolution, Institute of Geology and  
9 Geophysics, Chinese Academy of Sciences, Beijing 100029, China

10 2 State Key Laboratory of Palaeobiology and Stratigraphy, Nanjing Institute of  
11 Geology and Palaeontology, Chinese Academy of Sciences, Nanjing 210008, China

12 3 College of Earth Sciences, University of Chinese Academy of Sciences, Beijing  
13 100049, China

14 4 NERC Isotope Geosciences Laboratory, British Geological Survey, Keyworth NG12  
15 5GG, UK

16 5 Beihai Marine Station of Evo-Devo Institute, Nanjing University, Nanjing 210023,  
17 China

18  
19 ORCiDs: C. Y., 0000-0001-5224-8081; D. J. C., 0000-0002-9082-3283

20 \*Correspondence: [lixh@gig.ac.cn](mailto:lixh@gig.ac.cn)

21 Short title for the running headlines: Zircon U-Pb age of the Chengjiang biota  
22  
23

24 **Abstract**

25 The Cambrian Chengjiang biota of South China provided compelling fossil  
26 evidence for the rapid appearance of metazoan phyla in the Earth history (“Cambrian  
27 explosion”). However, the timing of the Chengjiang biota is poorly constrained due to  
28 lack of dateable rock materials within the Maotianshan Shale that yields the fossils.  
29 Here we integrate SIMS and CA-ID-TIMS U-Pb analyses of detrital zircons from the  
30 Maotianshan Shale to provide high precision geochronological constraint on the  
31 Chengjiang biota. The youngest group of SIMS U-Pb detrital zircon dates yields an  
32 age peak at 520 Ma. Six zircons from this group are further dated by CA-ID-TIMS  
33 U-Pb technique, but suggesting that they were not formed from a single zircon growth  
34 event. Thereby neither the age peak nor the weighted mean age defined by the  
35 youngest SIMS U-Pb dates could represent the maximum depositional age of  
36 Maotianshan Shale. Instead, the youngest CA-ID-TIMS U-Pb date,  $518.03 \pm$   
37  $0.69/0.71$  Ma ( $2\sigma$ , analytical uncertainty/incorporates U-Pb tracer calibration  
38 uncertainty), provides the first robust maximum age of the Chengjiang biota. This  
39 new geochronological constraint on the Chengjiang biota indicates that the Cambrian  
40 explosion reached its major phase around  $518.03 \pm 0.69/0.71$  Ma, demonstrating a  
41 protracted process ( $> 22$  myr) of the Cambrian explosion.

42

43

44 The Chengjiang biota from the Cambrian Maotianshan Shale Member of the  
45 Yu'an-shan Formation in South China, characterized by exceptionally well-preserved  
46 soft-bodied and weakly biomineralized fossils, shows the major phase of the  
47 Cambrian explosion of metazoans (e.g., [Chen et al. 1996](#); [Li et al. 2007](#); [Shu 2008](#);  
48 [Zhang & Shu 2014](#)). This biota contains nearly all the present animal phyla including  
49 Chordata (e.g., [Chen et al. 1999](#); [Shu et al. 1999](#); [Hou et al. 2017](#)), providing a unique  
50 window into metazoan diversity and ecosystems in the early Cambrian Period ([Zhao](#)  
51 [et al. 2010, 2012](#)). Although it has been studied more than 30 years, there is no high  
52 precision geochronological constraint on the Chengjiang biota. The current Cambrian  
53 chronostratigraphic model does not help to provide direct age constraint on the  
54 Chengjiang biota either ([Peng et al. 2012](#)), ultimately hampering to estimate the rate  
55 of the Cambrian explosion process.

56 Owing to the lack of ash bed in the Yu'an-shan Formation, several Rb-Sr, Ar-Ar and  
57 Pb-Pb analyses were conducted on the whole-rock and illite samples to directly  
58 determine the depositional age. These dating results range from ca. 560 Ma to ca. 534  
59 Ma with large analytical errors (e.g., [Chen et al. 2001](#); [Chang et al. 2004](#)). A SHRIMP  
60 (Sensitive High Resolution Ion Microprobe) zircon U-Pb age of  $526.5 \pm 1.1$  Ma has  
61 been determined from an ash bed at the bottom of the underlying Shiyantou  
62 Formation ([Fig. 1](#); [Compston et al. 2008](#)), providing the lower bracket of the age of  
63 Chengjiang biota. A breakthrough was made in recent years by analysing SIMS  
64 (Secondary Ion Mass Spectrometry) U-Pb ages of detrital zircons from basal  
65 Shiyantou Formation to the Maotianshan Shale Member, and the results demonstrate  
66 that the maximum age for the deposition of the Maotianshan Shale is  $\sim 520$  Ma  
67 ([Hofmann et al. 2016](#)). However, taking into account of an external uncertainty of 1%  
68 (2 SD) for SIMS zircon U-Pb technique (e.g., [Ireland & Williams 2003](#)), the age

69 constraint on the Chengjiang biota needs to be refined further. Here we aim to get the  
70 high precision geochronological constraint on the Chengjiang biota using an  
71 integrated approach that includes SIMS and CA-ID-TIMS (Chemical  
72 Abrasion-Isotope Dilution-Thermal Ionization Mass Spectrometry) zircon U-Pb  
73 analytical methods. Our new results demonstrate that the age of the Chengjiang biota  
74 is not earlier than  $518.03 \pm 0.69/0.71$  Ma, and the Cambrian explosion may have  
75 lasted more than 22 million years.

76

### 77 **Geological background and sampling**

78 The early Cambrian Chengjiang biota occurs in the Maotianshan Shale Member of  
79 the Yu'an-shan Formation in eastern Yunnan Province, South China (Fig. 1). It has  
80 been discovered at numerous localities in eastern Yunnan Province, and the  
81 best-preserved fossils and quarries occur in Chengjiang-Haikou-Anning areas (Zhao  
82 *et al.* 2010). The studied Xiaolantian section is located about 6 km to the east of  
83 Chengjiang County town, and about 3 km away from the Maotianshan section where  
84 the Chengjiang biota was first discovered (Fig. 1).

85 The early Cambrian succession of the Xiaolantian section deposited in a shallow  
86 marine setting includes upward in order the Zhujiaping, Shiyantou, and Yu'an-shan  
87 formations (Fig. 1; Zhu *et al.* 2001). The Zhujiaping Formation consists of three  
88 members in eastern Yunnan Province, upward in order, Daibu, Zhongyicun and Dahai  
89 members. In the Xiaolantian section, the Daibu Member is composed predominately  
90 of cherty dolostone. The Zhongyicun Member measures 37 meters thick and is  
91 composed of dolomitic phosphate with interlayered phosphate. The Dahai Member is  
92 absent in this section. Unconformably overlying the Zhujiaping Formation is the  
93 Shiyantou Formation, which is about 52 meters thick and consists of siltstone. The

94 Yu'anshan Formation is 170 meters thick and consists of three members, namely the  
95 lower Black Shale Member, the middle Maotianshan Shale Member, and the upper  
96 Siltstone Member (Zhao *et al.* 2012). Regional stratigraphic correlation indicates that  
97 *Anabarites trisulcatus-Protohertzina anabarica* Assemblage Zone and *Paragloborilus*  
98 *subglobosus-Purella squamulosa* Assemblage Zone occur in the Daibu-lower middle  
99 Zhongyicun members and the upper Zhongyicun Member, respectively (Fig. 1; Yang  
100 *et al.* 2014, 2016a). *Sinosachites flabelliformis-Tannuolina zhangwentangi*  
101 Assemblage Zone occurs in the upper part of the Shiyantou Formation, and extends to  
102 the basal Yu'anshan formations; *Parabadiella* Zone occurs in the lower Yu'anshan  
103 Formation and *Eoredlichia-Wutingaspis* Zone occurs in the overlying Maotianshan  
104 Shale Member (Fig. 1; Zhu *et al.* 2001; Steiner *et al.* 2007; Yang *et al.* 2014, 2016a).  
105 Two SIMS zircon U-Pb ages of  $535.2 \pm 1.7$  Ma and  $526.5 \pm 1.1$  Ma have been dated  
106 from ash beds in the middle Zhongyicun Member and at the base of the Shiyantou  
107 Formation in the Meishucun section in the same area, respectively (Fig. 1; Compston  
108 *et al.* 2008; Zhu *et al.* 2009).

109 Two samples (14CJ-2 and 14CJ-3) from the lower part of Maotianshan Shale  
110 Member in the Xiaolantian section ( $24^{\circ}40'53''\text{N}$ ,  $102^{\circ}58'50''\text{E}$ ) were collected for  
111 SIMS and CA-ID-TIMS zircon U-Pb dating (Fig. 1). Sample 14CJ-2 is a fine-grained  
112 siltstone, and sample 14CJ-3 is a mudstone which locates about 60 cm above 14CJ-2  
113 (Fig. 2).

114

### 115 **Zircon U-Pb dating methods**

116 Separated zircon crystals were mounted in an epoxy resin together with zircon  
117 standards Plešovice, 91500, Penglai and Qinghu. All zircon grains were documented  
118 with transmitted and reflected light photomicrographs and cathodoluminescence

119 images to reveal their external and internal structures, and the mount was  
120 vacuum-coated with high-purity gold prior to SIMS U-Pb analysis. Measurements of  
121 U, Th and Pb isotopes were conducted using a Cameca 1280HR SIMS at the Institute  
122 of Geology and Geophysics, Chinese Academy of Sciences. A single electron  
123 multiplier was used in ion-counting mode to measure secondary ion beam intensities  
124 by peak jumping. Each measurement consists of 7 cycles, and the total analytical time  
125 is about 12 minutes. Detailed SIMS zircon U-Pb analytical method is described by Li  
126 *et al.* (2009). Analyses of standard zircon grains were interspersed with those  
127 unknown grains. A long-term uncertainty of 1.5% (1 RSD) for  $^{206}\text{Pb}/^{238}\text{U}$   
128 measurements of the standard zircon was propagated to the unknowns (Li *et al.* 2010),  
129 because all the analysed grains are detrital zircons. U-Th-Pb ratios were determined  
130 relative to the Plešovice standard zircon (Sláma *et al.* 2008), and the absolute  
131 abundances were calibrated to the standard zircon 91500 (Wiedenbeck *et al.* 1995).  
132 Measured Pb isotopic compositions were corrected for common Pb using the  
133  $^{204}\text{Pb}$ -method. Corrections are sufficiently small to be insensitive to the choice of  
134 common Pb composition. An average of present-day crustal composition (Stacey &  
135 Kramers 1975) is used for the common Pb assuming that the common Pb is largely  
136 surface contamination introduced during sample preparation. Data reduction was  
137 carried out using the Isoplot/Exv. 4.15. More details for calibration methods are  
138 described by Li *et al.* (2009). In order to monitor the external uncertainties of SIMS  
139 U-Pb measurements, analyses of zircon standard Qinghu were interspersed with  
140 unknowns. 20 analyses yielded a weighted mean  $^{238}\text{U}$ - $^{206}\text{Pb}$  age of  $159.4 \pm 1.1$  Ma  
141 (MSWD = 0.44, 95% confidence interval), identical within errors to the reported age  
142 of  $159.5 \pm 0.2$  Ma (Li *et al.* 2013).

143 Zircons of the youngest  $^{238}\text{U}$ - $^{206}\text{Pb}$  date population were micro-drilled off from the

144 SIMS mount for CA-ID-TIMS analysis in the NERC Isotope Geosciences Laboratory  
145 (NIGL), British Geological Survey. Zircons were annealed in a muffle furnace at  
146 900°C for ~60 hours in quartz beakers before being transferred to 3 ml Hex Savillex  
147 beakers. After ultrasonic bath and rinsing by 30% HNO<sub>3</sub>, zircons were transferred to  
148 300 µl Teflon PFA microcapsules, leached in ~5:1 mix of 29M HF + 30% HNO<sub>3</sub> for  
149 12 hours at 180°C (Mattinson 2005). Then the acid solution was removed, and zircons  
150 were rinsed again by 30% HNO<sub>3</sub> and 6M HCl before spiking with the mixed  
151 EARTHTIME <sup>235</sup>U-<sup>233</sup>U-<sup>205</sup>Pb tracer (Condon *et al.* 2015). The single zircons were  
152 dissolved in ~ 120 µl of 29M HF with a trace amount of 30% HNO<sub>3</sub> at 220°C for 48  
153 hours. After converting the dried fluorides into chlorides in 3M HCl at ~180°C  
154 overnight, U and Pb were separated using standard HCl-based anion-exchange  
155 chromatographic procedures on 0.05 ml PTFE columns. Pb and U were loaded  
156 together on a single Re filament in a silica-gel/phosphoric acid mixture, and analysed  
157 by the Thermo-Electron Triton Thermal Ionisation Mass-Spectrometer in NIGL. Pb  
158 isotopes were measured by peak-hopping on a single SEM detector. U isotope  
159 measurements were made in static Faraday mode or on a single SEM detector, based  
160 on the uranium content. Age calculations and uncertainty estimation were made using  
161 the Tripoli and ET\_Redux (Bowring *et al.* 2011).

162 Both SIMS and CA-ID-TIMS U-Pb dates are calculated using the <sup>238</sup>U and <sup>235</sup>U  
163 decay constants of Jaffey *et al.* (1971). SIMS and CA-ID-TIMS zircon U-Pb data are  
164 given in the Appendix Table 1 and Table 2, respectively, and uncertainties on  
165 individual analysis are reported at 2σ level in the main text. The CA-ID-TIMS  
166 <sup>238</sup>U-<sup>206</sup>Pb date uncertainties are presented as ± X/Y in this study, where X is the  
167 uncertainty arising solely from internal or analytical uncertainty, and Y includes X and  
168 the tracer calibration uncertainty. The systematic uncertainty associated with <sup>238</sup>U

169 decay constant also needs to be propagated if it is compared with other chronometers  
170 such as Ar-Ar or astrochronology. For interpretation of the zircon ages only  
171 concordant or nearly concordant (<10% discordant) data were included. The measured  
172  $^{207}\text{Pb}$ - $^{206}\text{Pb}$  and  $^{238}\text{U}$ - $^{206}\text{Pb}$  dates are used for zircons older and younger than 1000 Ma,  
173 respectively, for plotting the zircon age probability histograms.

174

## 175 **Results**

### 176 *SIMS zircon U-Pb results*

177 Zircons from sample 14CJ-2 are 70-120  $\mu\text{m}$  in length and have aspect ratios of  
178 1-3. Most of them are euhedral and subhedral in morphology, with a small portion of  
179 rounded grains. Except for a few grains showing no oscillatory zoning, most zircons  
180 have oscillatory zoning under CL images. Th/U ratios of the analysed zircons range  
181 from 0.22 to 3.92 (mostly within 0.22-2.06). These features indicate that nearly all the  
182 analysed zircons are of magmatic origin (Fig. 3). Of the 113 analyses on 113 zircons  
183 from this sample, 99 are concordant within uncertainties. The measured  $^{238}\text{U}$ - $^{206}\text{Pb}$  (<  
184 1000 Ma) and  $^{207}\text{Pb}$ - $^{206}\text{Pb}$  (> 1000 Ma) dates range from  $492 \pm 14$  Ma to  $3083 \pm 10$   
185 Ma. Apart from the youngest date which is a little discordant ( $492 \pm 14$  Ma,  
186 discordance = 6.1%), the youngest population includes four dates, namely  $515 \pm 14$   
187 Ma,  $518 \pm 16$  Ma,  $524 \pm 16$  Ma and  $528 \pm 16$  Ma, forming a peak at 520 Ma. Other  
188 four older age peaks are present at ca. 605 Ma, ca. 800 Ma, ca. 1025 Ma and ca. 2510  
189 Ma (Fig. 4a).

190 Zircons from sample 14CJ-3 are similar with those from 14CJ-2. Thirty-nine zircon  
191 U-Pb dates out of 43 analyses are concordant within uncertainty. The measured  
192  $^{238}\text{U}$ - $^{206}\text{Pb}$  (< 1000 Ma) and  $^{207}\text{Pb}$ - $^{206}\text{Pb}$  (> 1000 Ma) dates range from  $499 \pm 14$  Ma to  
193  $2570 \pm 18$  Ma. They form the main peak at ca. 765 Ma, with a subordinate age peak at

194 ca. 960 Ma and one “broad” age group between  $499 \pm 14$  Ma and  $592 \pm 18$  Ma (Fig.  
195 4b). The two youngest  $^{238}\text{U}$ - $^{206}\text{Pb}$  dates are  $499 \pm 14$  Ma (z37) and  $518 \pm 16$  Ma (z07).

196

### 197 *ID-TIMS zircon U-Pb results*

198 Five crack-free, inclusion-free, and texture uncomplicated zircons from the  
199 youngest populations of the two samples and one grain from sample LM-23-12 in  
200 Hofmann *et al.* (2016) were further dated by CA-ID-TIMS U-Pb method. Except for  
201 the grain 14CJ-3 z37 with very high Pbc (= 24.9 pg), other five grains yield useful  
202 dates. The  $^{238}\text{U}$ - $^{206}\text{Pb}$  dates of analysed zircons 14CJ-2 z02, 14CJ-2 z29, 14CJ-2 z66,  
203 14CJ-3 z07, and LM-23-12 z45 are  $524.33 \pm 0.86/0.87$  Ma,  $527.79 \pm 2.50/2.51$  Ma,  
204  $584.42 \pm 1.23/1.24$  Ma,  $518.03 \pm 0.69/0.71$  Ma, and  $544.41 \pm 4.21/4.21$  Ma,  
205 respectively (Fig. 3, 5). They corroborate and refine the SIMS dates except for 14CJ-2  
206 z66, whose SIMS date is a little discordant and unreliable (discordance = 6.1%). The  
207 youngest zircon 14CJ-3 z07 has low common Pb (Pbc = 0.28 pg), and its U-Pb date is  
208 concordant (discordance = -0.7%), indicating that its  $^{238}\text{U}$ - $^{206}\text{Pb}$  date,  $518.03 \pm$   
209  $0.69/0.71$  Ma, is highly reliable (Fig. 5).

210

## 211 **Discussion**

### 212 *Maximum age of the Chengjiang biota*

213 When interpreting the detrital zircon dates, only U-Pb data within analytical  
214 uncertainty of concordia should be used. A percentage date difference discordance  
215 filter, such as 10%, is often applied to categorize zircon U-Pb dataset. In this study, all  
216 the zircons of the youngest SIMS U-Pb date population pass the 10% discordance  
217 filter. However, zircon grain 14CJ-2 z66 with the youngest SIMS U-Pb date ( $492 \pm 14$   
218 Ma) of sample 14CJ-2 has a discordance of 6.1% (Fig. 2), and its CA-ID-TIMS U-Pb

219 date is  $584.42 \pm 1.23/1.24$  Ma which is significantly older than its SIMS U-Pb date,  
220 indicating that the extremely young SIMS U-Pb date of this grain results from Pb-loss  
221 (Fig. 5). Similarly, the grain 14CJ-3 z37 with the youngest SIMS U-Pb date ( $499 \pm 14$   
222 Ma) of sample 14CJ-3 has a discordance of 7.5%, and it incorporates high common  
223 Pb (= 24.9 pg), implying that its young SIMS U-Pb date is probably also caused by  
224 Pb-loss (Fig. 5). Consequently, the SIMS U-Pb results of grains 14CJ-2 z66 and  
225 14CJ-3 z37 are not included in the following discussion.

226 There are several different strategies to constrain the maximum depositional ages of  
227 strata containing detrital zircons, such as the youngest single grain age, the youngest  
228 graphical age peak controlled by more than one single grain age, the weighted mean  
229 age of the youngest two or more grains with overlapping  $1\sigma$  uncertainties, and the  
230 weighted mean age of youngest three or more grains that overlap in age at  $2\sigma$   
231 uncertainties (e.g., Dickinson & Gehrels 2009). Defining the maximum depositional  
232 age by the youngest age peak or a weighted mean age yielded from the youngest  
233 detrital zircon population has an assumption that those zircons are from a single  
234 zircon growth event. This assumption is not true for most sedimentary rocks. In this  
235 study, the youngest detrital zircon SIMS U-Pb age peak is ca. 520 Ma, and their  
236 weighted mean age is  $520.3 \pm 6.7$  Ma ( $2\sigma$ ,  $n = 5$ , MSWD = 0.5). The normal  
237 distribution pattern (Fig. 4) and the acceptable MSWD value of the weighted mean  
238 age (Fig. 5) imply that those zircons probably are from a single zircon growth event.  
239 However, the three CA-ID-TIMS U-Pb dates of zircons from this group are  $524.33 \pm$   
240  $0.86/0.87$  Ma,  $527.79 \pm 2.50/2.51$  Ma, and  $518.03 \pm 0.69/0.71$  Ma. They are not  
241 overlapping with each other within  $2\sigma$  uncertainties (Fig. 5), and the MSWD value of  
242 their weighted mean age is extremely high, indicating that they are not from a single  
243 zircon growth event. Therefore none of the youngest age peak or the weighted mean

244 age defined by the youngest SIMS U-Pb population is meaningful and suitable to  
245 define the maximum depositional age.

246 In theory, using the youngest concordant zircon U-Pb date is the best strategy to  
247 constrain the maximum depositional age (e.g., [Spencer et al. 2016](#)). However, Pb-loss,  
248 common Pb incorporation, discordance, and analytical uncertainty would compromise  
249 this strategy, especially for the *in situ* SIMS and LA-ICPMS zircon U-Pb datasets.  
250 CA-ID-TIMS zircon U-Pb technique is capable of removing zircon domains that  
251 suffered Pb-loss, and yields the most precise and accurate U-Pb dates (e.g., [Mattinson](#)  
252 [2005](#)). Therefore the youngest concordant CA-ID-TIMS U-Pb date of detrital zircons  
253 provides the most robust constraint on the maximum depositional age. However, the  
254 time-consuming character of the CA-ID-TIMS zircon U-Pb method makes it  
255 impractical to date a large number of detrital zircons to determine the youngest U-Pb  
256 date. SIMS U-Pb analysis of zircon is efficient and accurate with an external error of  
257 approximately 1%, and its “undamaged” analytical character makes it possible to  
258 perform the CA-ID-TIMS U-Pb analysis on the same zircon grain after SIMS U-Pb  
259 dating. As a result, integrating SIMS and CA-ID-TIMS zircon U-Pb techniques is the  
260 most promising method to constrain the depositional age of strata (e.g., [Yang et al.](#)  
261 [2017b](#)), especially for those lacking ash bed interlayers.

262 SIMS U-Pb dating results in this study demonstrate that the youngest  $^{238}\text{U}$ - $^{206}\text{Pb}$   
263 date peak of detrital zircons from the Maotianshan Shale samples 14CJ-2 and 14CJ-3  
264 is ca. 520 Ma ([Fig. 4](#)), which also are confirmed with the results of [Hofmann et al.](#)  
265 [\(2016\)](#). Six zircons of the youngest SIMS U-Pb group are further dated by  
266 CA-ID-TIMS, yielding five useful U-Pb dates. They are not from a single zircon  
267 growth event as discussed above. The youngest CA-ID-TIMS  $^{238}\text{U}$ - $^{206}\text{Pb}$  date,  $518.03$   
268  $\pm 0.69/0.71$  Ma, provides the maximum depositional age of the sampling horizon in

269 the Maotianshan Shale, i.e., the maximum age of the Chengjiang biota. However, it  
270 should also be noted that the possibility of underestimating the maximum depositional  
271 age cannot be excluded because of possible Pb-loss even the zircon has been chemical  
272 abraded. Petrographic and geochemical analyses indicate that the provenance of the  
273 Maotianshan Shale was a recycled orogen overall, and it was less mature and included  
274 minor elements commonly associated with mafic sources (Hofmann *et al.* 2016). The  
275 characters of sedimentary provenance imply that sediments of the Xiaolantian section  
276 were possible to accumulate contemporary volcanic material, so that the sedimentary  
277 age of the Maotianshan Shale is likely close to the youngest zircon U-Pb date  $518.03$   
278  $\pm 0.69/0.71$  Ma determined by CA-ID-TIMS. A  $^{207}\text{Pb}$ - $^{206}\text{Pb}$  date of  $517.0 \pm 1.5$  Ma on  
279 the *Antatlasia gutta-pluviae* Zone (trilobites) of Morocco (Landing *et al.* 1998)  
280 probably constrains the minimum age of the Chengjiang biota based on the global  
281 biostratigraphic correlations (e.g., Peng *et al.* 2012; Yang *et al.* 2016b; Zhang *et al.*  
282 2017). The new geochronological constraint confirms a Cambrian Age 3 depositional  
283 age for the Maotianshan Shale in Yunnan Province and is consistent with global  
284 chronostratigraphic correlation (Zhu *et al.* 2006, 2010).

285

### 286 ***Geochronological constraint on the major phase of Cambrian explosion***

287 The Cambrian explosion delineates the unprecedented, unique evolutionary event  
288 that nearly all metazoan phyla made their first appearances in the fossil record in a  
289 relatively short time span during the Ediacaran-Cambrian transition, leading to the  
290 establishment of metazoan-dominated ecosystem accompanied by widespread  
291 biomineralization, as well as increases of size and morphological disparity among  
292 metazoan phyla (Zhang & Shu 2014). The diversification of coelomates that produced  
293 deep and complex burrows marks the first major stage of the Cambrian explosion,

294 which corresponds to the base of the Cambrian System ([Landing et al. 2013](#)).  
295 However, molecular clock studies demonstrate that the common ancestor of all  
296 metazoans originated prior to ca. 800 Ma with the bilaterians diversified at least 100  
297 Ma before the Cambrian Period (e.g., [dos Reis et al. 2015](#)). In the perspective of fossil  
298 records, some complex trace fossils such as *Treptichnus*, Cambrian-type skeletal  
299 fossils such as *Anabarites* and *Cambrotubulus*, and the oldest triploblastic bilaterian  
300 *Kimberella* start their appearances before the Cambrian Period as well ([Jensen et al.](#)  
301 [2000](#); [Gehling et al. 2001](#); [Macdonald et al. 2014](#); [Zhu et al. 2017](#)). Both the  
302 molecular clock studies and fossil records imply a deep root for the Cambrian  
303 explosion of metazoans ([Zhu et al. 2017](#)).

304 The arthropods are the most diverse representatives of the Cambrian biotas younger  
305 than 520 Ma such as the Chengjiang biota (e.g., [Li et al. 2007](#); [Zhao et al. 2010](#)). The  
306 trilobites form a clade in cladistic analyses of the Arthropoda ([Wills et al. 1994](#)). Thus,  
307 the first trilobite occurrence is a key biotic event in the Cambrian biostratigraphy and  
308 marks the most dramatic event in the modernization of ecologic communities in the  
309 Cambrian explosion, i.e. the onset of the major phase of the Cambrian explosion  
310 ([Zhang et al. 2014, 2017](#)). Also, the first appearance of trilobites has long been  
311 considered as the primary indicator to define the base of Cambrian Series 2 and Stage  
312 3 ([Peng et al. 2012](#); [Zhang et al. 2017](#) for reviews). However, the first appearances of  
313 trilobites are endemic and diachronous on separate paleocontinents ([Landing et al.](#)  
314 [2013](#); [Zhang et al. 2017](#)). Geochronological constraints on the first appearances of  
315 trilobites are scarce. Zircon U-Pb age of  $520.93 \pm 0.14$  Ma from the upper part of the  
316 Lie de vin Formation in Morocco ([Malloof et al. 2010](#)) provides a maximum  
317 geochronological constraint on the first determinable trilobite in this region ([Geyer &](#)  
318 [Landing 2006](#)). The first determinable trilobites in Avalonia including the olenelloid

319 *Callavia broeggeri*, which are relatively late among the early trilobites (Landing *et al.*  
320 2013), are roughly constrained by an zircon U-Pb age of  $519.30 \pm 0.23$  Ma from the  
321 Caerfai Bay Shales Formation in Wales (Harvey *et al.* 2011). Collectively, the  
322 occurrence of the first trilobites is possibly bracketed between  $520.93 \pm 0.14$  Ma and  
323  $519.30 \pm 0.23$  Ma.

324 Generic diversity of South China indicates that metazoan diversity received the  
325 most significant boost in the middle Cambrian Age 3 due to the exceptional  
326 Chengjiang biota (Li *et al.* 2007), which is consistent with the global biodiversity data  
327 (Na & Kiessling 2015). Hosting 228 species in over 18 phyla of animals and  
328 displaying the well establishment of the modern style of the complex marine  
329 community (Fig. 6; Li *et al.* 2007; Zhao *et al.* 2010; Zhang & Shu 2014), the  
330 Chengjiang biota provides a unique window to show the major phase of the Cambrian  
331 explosion (Fig. 6). The maximum age of the Chengjiang biota is constrained at  $518.03$   
332  $\pm 0.69/0.71$  Ma, implying that the Cambrian explosion is a protracted evolutionary  
333 process (Erwin *et al.* 2011; Shu *et al.* 2014; Zhang & Shu 2014) which takes more  
334 than 22 million years. The onset of the major phase of Cambrian explosion is marked  
335 by the global first appearance of trilobites which is possibly bracketed between  $520.93$   
336  $\pm 0.14$  Ma and  $519.30 \pm 0.23$  Ma. The major phase of Cambrian explosion represents  
337 a rapid episode of metazoan diversification in a relatively short time interval. This  
338 phase is followed by a diversity decline in Cambrian Age 4 which extended further  
339 through the rest of the Cambrian Period (Li *et al.* 2007; Na & Kiessling 2015).

340

## 341 **Conclusions**

342 We performed integrated SIMS and CA-ID-TIMS U-Pb dating on the detrital  
343 zircons from the Maotianshan Shale Member which yields the Chengjiang biota in

344 South China. The youngest detrital zircon population defines a SIMS U-Pb age peak  
345 at ca. 520 Ma. CA-ID-TIMS U-Pb dates of these zircons are scattered with the  
346 youngest concordant one at  $518.03 \pm 0.69/0.71$  Ma, providing a maximum age for the  
347 Chengjiang biota. The new geochronological constraint on the Chengjiang biota  
348 indicates that the Cambrian explosion is a gradual and protracted evolutionary process,  
349 along with a rapid episode of metazoan diversification at around  $518.03 \pm 0.69/0.71$   
350 Ma.

351

### 352 **Acknowledgements**

353 We thank Qiu-Li Li, Yu Liu, Guo-Qiang Tang, Xiao-Xiao Ling, and Nicola  
354 Atkinson for assistance in SIMS and CA-ID-TIMS zircon U-Pb analyses, Zhongwu  
355 Lan and Zhi Chen for field assistance. In addition, we owe great thanks to professors  
356 Xingliang Zhang and Jahandar Ramezani for insightful and constructive comments on  
357 this manuscript.

358

### 359 **Funding**

360 This work was funded by the Strategic Priority Research Program (B) of the  
361 Chinese Academy of Sciences (grant XDB18030300) and the Chinese Ministry of  
362 Science and Technology (grant 2013CB835000).

363

### 364 **References**

- 365 Bowring, J. F., McLean, N. M. & Bowring, S. A. 2011. Engineering cyber  
366 infrastructure for U-Pb geochronology: Tripoli and U-Pb\_Redux. *Geochemistry,*  
367 *Geophysics, Geosystems*, 12(6), Q0AA19,  
368 <http://dx.doi.org/10.1029/2010GC003479>.  
369 Chang, X. Y., Chen, L. Z., Hu, S. X., Wang, J. H. & Zhu, B. Q. 2004. Pb-Pb isotope  
370 dating of the Chengjiang Fauna-bearing beds. *Acta Geoscientica Sinica*, 25(2),

371 181-184 (in Chinese with English abstract).

372 Chen, J. Y., Zhou, G. Q., Zhu, M. Y. & Yeh, K. Y. 1996. The Chengjiang biota: A  
373 unique window of the Cambrian Explosion. National Museum of Natural Science,  
374 Taichung (Taiwan), p.1-222.

375 Chen, J. Y., Huang, D. Y. & Li, C. W. 1999. An early Cambrian craniate-like chordate.  
376 Nature, 402, 518-522, <http://dx.doi.org/10.1038/990080>.

377 Chen, L. Z., Jiang, Z. W., Luo, H. L., Yin, J. Y. & Hu, S. X. 2001.  $^{40}\text{Ar}$ - $^{39}\text{Ar}$  age  
378 spectrum of Chengjiang Fauna horizon. Yunnan Geology, 20(3), 289-296 (in  
379 Chinese with English abstract).

380 Cohen, K. M., Finney, S. C., Gibbard, P. L. & Fan, J. X. 2013. The ICS International  
381 Chronostratigraphic Chart. Episodes, 36(3), 199-204.

382 Compston, W., Zhang, Z. C., Cooper, J. A., Ma, G. G. & Jenkins, R. J. F. 2008. Further  
383 SHRIMP geochronology on the early Cambrian of South China. American Journal  
384 of Science, 308(4), 399-420, <http://dx.doi.org/10.2475/04.2008.01>.

385 Condon, D. J., Schoene, B., McLean, N. M., Bowring, S. A. & Parrish, R. R. 2015.  
386 Metrology and traceability of U-Pb isotope dilution geochronology  
387 (EARTHTIME Tracer Calibration Part I). Geochimica et Cosmochimica Acta, 164,  
388 464-480, <http://dx.doi.org/10.1016/j.gca.2015.05.026>.

389 Dickinson, W. R. & Gehrels, G. E. 2009. Use of U-Pb ages of detrital zircons to infer  
390 maximum depositional ages of strata: a test against a Colorado Plateau Mesozoic  
391 database. Earth and Planetary Science Letters, 288, 115-125,  
392 <https://doi.org/10.1016/j.epsl.2009.09.013>.

393 dos Reis, M., Thawornwattana, Y., Angelis, K., Telford, M.J., Donoghue, P.C.J. &  
394 Yang, Z. 2015. Uncertainty in the timing of origin of animals and the limits of  
395 precision in molecular timescales. Current Biology, 25, 2939-2950,  
396 <http://dx.doi.org/10.1016/j.cub.2015.09.066>.

397 Erwin, D. H., Laflamme, M., Tweedt, S. M., Sperling, E. A., Pisani, D. & Peterson, K.  
398 J. 2011. The Cambrian conundrum: early divergence and later ecological success  
399 in the early history of animals. Science, 334, 1091-1097,  
400 <https://doi.org/10.1126/science.1206375>.

401 Gehling, J. G., Jensen, S., Droser, M. L., Myrow, P. M. & Narbonne, G. M. 2001.  
402 Burrowing below the basal Cambrian GSSP, Fortune Head, Newfoundland.  
403 Geological Magazine, 138(2), 213-218,  
404 <https://doi.org/10.1017/S001675680100509X>.

405 Geyer, G. & Landing, E. 2006. Latest Ediacaran and Cambrian of the Moroccan Atlas  
406 regions. In: Geyer, G., Landing, E. (Eds.), Morocco 2006. Ediacaran-Cambrian  
407 Depositional Environments and Stratigraphy of the Western Atlas Regions.  
408 Explanatory Description and Field Excursion Guide: Beringeria Special Issue, 6,  
409 9-75.

410 Harvey, T. H., Williams, M., Condon, D. J., Wilby, P. R., Siveter, D. J., Rushton, A. W.,  
411 Leng, M. J. & Gabbott, S. E. 2011. A refined chronology for the Cambrian  
412 succession of southern Britain. *Journal of the Geological Society*, 168(3), 705-716,  
413 <https://doi.org/10.1144/0016-76492010-031>.

414 Hofmann, M. H., Li, X. H., Chen, J. Y., MacKenzie, L. A. & Hinman, N. W. 2016.  
415 Provenance and temporal constraints of the Early Cambrian Maotianshan Shale,  
416 Yunnan Province, China. *Gondwana Research*, 37, 348-361.  
417 <http://dx.doi.org/10.1016/j.gr.2015.08.015>.

418 Hou, X. G., Siveter, D. J., Siveter, D. J., Aldridge, R. J., Cong, P. Y., Gabbott, S. E.,  
419 Ma, X. Y., Purnell, M. A. & Williams, M. 2017. The Cambrian fossils of  
420 Chengjiang, China: the flowering of early animal life (second edition). John Wiley  
421 & Sons, p. 1-315.

422 Ireland, T. R. & Williams, I. S. 2003. Considerations in zircon geochronology by  
423 SIMS, in *Zircon*, edited by J.M. Hanchar & P.W.O. Hoskin, *Reviews in*  
424 *Mineralogy and Geochemistry*, 53, 215-241, <https://doi.org/10.2113/0530215>.

425 Jaffey, A. H., Flynn, K. F., Glendenin, L. E., Bentley, W. T. & Essling, A. M. 1971.  
426 Precision measurement of half-lives and specific activities of U235 and U238.  
427 *Physical Review C*, 4(5), 1889, <https://doi.org/10.1103/PhysRevC.4.1889>.

428 Jensen, S., Saylor, B. Z., Gehling, J. G. & Germs, G. J. 2000. Complex trace fossils  
429 from the terminal Proterozoic of Namibia. *Geology*, 28(2), 143-146,  
430 [http://dx.doi.org/10.1130/0091-7613\(2000\)28<143:CTFFTT>2.0.CO;2](http://dx.doi.org/10.1130/0091-7613(2000)28<143:CTFFTT>2.0.CO;2).

431 Landing, E., Bowring, S. A., Davidek, K. L., Westrop, S. R., Geyer, G. & Heldmaier,  
432 W. 1998. Duration of the Early Cambrian: U-Pb ages of volcanic ashes from  
433 Avalon and Gondwana. *Canadian Journal of Earth Sciences*, 35(4), 329-338,  
434 <https://doi.org/10.1139/e97-107>.

435 Landing, E., Geyer, G., Brasier, M. D. & Bowring, S. A. 2013. Cambrian evolutionary  
436 radiation: context, correlation, and chronostratigraphy-overcoming deficiencies of  
437 the first appearance datum (FAD) concept. *Earth-Science Reviews*, 123, 133-172,  
438 <http://dx.doi.org/10.1016/j.earscirev.2013.03.008>.

- 439 Li, G. X., Steiner, M., Zhu, X. J., Yang, A. H., Wang, H. F. & Erdtmann, B. D. 2007.  
440 Early Cambrian metazoan fossil record of South China: Generic diversity and  
441 radiation patterns. *Palaeogeography, Palaeoclimatology, Palaeoecology*, 254,  
442 229-249, <http://dx.doi.org/10.1016/j.palaeo.2007.03.017>.
- 443 Li, Q. L., Li, X. H., Liu, Y., Tang, G. Q., Yang, J. H. & Zhu, W. G. 2010. Precise U-Pb  
444 and Pb-Pb dating of Phanerozoic baddeleyite by SIMS with oxygen flooding  
445 technique. *Journal of Analytical Atomic Spectrometry*, 25(7), 1107-1113,  
446 <http://dx.doi.org/10.1039/b923444f>.
- 447 Li, X. H., Liu, Y., Li, Q. L., Guo, C. H. & Chamberlain, K. R. 2009. Precise  
448 determination of Phanerozoic zircon Pb/Pb age by multicollector SIMS without  
449 external standardization. *Geochemistry, Geophysics, Geosystems*, 10, Q04010,  
450 <http://dx.doi.org/10.1029/2009GC002400>.
- 451 Li, X. H., Tang, G. Q., Gong, B., Yang, Y. H., Hou, K. J., Hu, Z. C., Li, Q. L., Liu, Y.  
452 & Li, W. X. 2013. Qinghu zircon: a working reference for microbeam analysis of  
453 U-Pb age and Hf and O isotopes. *Chinese Science Bulletin*, 58(36), 4647-4654,  
454 <http://dx.doi.org/10.1007/s11434-013-5932-x>.
- 455 Macdonald, F. A., Pruss, S. B. & Strauss, J. V. 2014. Trace fossils with spreiten from  
456 the late Ediacaran Nama Group, Namibia: complex feeding patterns five million  
457 years before the Precambrian-Cambrian boundary. *Journal of Paleontology*, 88(2),  
458 299-308, <http://dx.doi.org/10.1666/13-042>.
- 459 Maloof, A. C., Ramezani, J., Bowring, S. A., Fike, D. A., Porter, S. M. & Mazouad, M.  
460 2010. Constraints on early Cambrian carbon cycling from the duration of the  
461 Nemakit-Daldynian-Tommotian boundary  $\delta^{13}\text{C}$  shift, Morocco. *Geology*, 38(7),  
462 623-626, <http://dx.doi.org/10.1130/G30726.1>.
- 463 Mattinson, J. M. 2005. Zircon U-Pb chemical abrasion ("CA-TIMS") method:  
464 combined annealing and multi-step partial dissolution analysis for improved  
465 precision and accuracy of zircon ages. *Chemical Geology*, 220, 47-66,  
466 <http://dx.doi.org/10.1016/j.chemgeo.2005.03.011>.
- 467 Na, L. & Kiessling, W. 2015. Diversity partitioning during the Cambrian radiation.  
468 *Proceedings of the National Academy of Sciences*, 112, 4702-4706,  
469 <https://doi.org/10.1073/pnas.1424985112>.
- 470 Peng, S. C., Babcock, L. E. & Cooper, R. A. 2012. The Cambrian Period. In:  
471 Gradstein, F. M., Ogg, J. G., Schmidtz, M. D. & Ogg, G. M. (Eds.), *The Geologic*  
472 *Time Scale 2012*, vol. 2. Elsevier BV, Amsterdam, p. 437-488.

473 <https://doi.org/10.1016/B978-0-444-59425-9.00019-6>.

474 Shu, D. G., Luo, H. L., Conway Morris, S., Zhang, X. L., Hu, S. X., Chen, L., Han, J.,  
475 Zhu, M., Li, Y. & Chen, L. Z. 1999. Lower Cambrian vertebrates from south  
476 China. *Nature*, 402, 42-46, <https://doi.org/10.1038/46965>.

477 Shu, D. G. 2008. Cambrian explosion: Birth of tree of animals. *Gondwana Research*,  
478 14, 219-240, <https://doi.org/10.1016/j.gr.2007.08.004>.

479 Sláma, J., Košler, J., Condon, D. J., Crowley, J. L., Gerdes, A., Hanchar, J. M.,  
480 Horstwood, M. S. A., Morris, G. A., Nasdala, L., Norberg, N., Schaltegger, U.,  
481 Schoene, B., Tubrett, M. N. & Whitehouse, M. J. 2008. Plešovice zircon - a new  
482 natural reference material for U-Pb and Hf isotopic microanalysis. *Chemical*  
483 *Geology*, 249, 1-35, <https://doi.org/10.1016/j.chemgeo.2007.11.005>.

484 Spencer, C. J., Kirkland, C. L. & Taylor, R. J. 2016. Strategies towards statistically  
485 robust interpretations of in situ U-Pb zircon geochronology. *Geoscience Frontiers*,  
486 7, 581-589, <http://dx.doi.org/10.1016/j.gsf.2015.11.006>.

487 Stacey, J. S. & Kramers, J. D. 1975. Approximation of terrestrial lead isotope  
488 evolution by a two-stage model. *Earth and Planetary Science Letters*, 26, 207-221,  
489 [https://doi.org/10.1016/0012-821X\(75\)90088-6](https://doi.org/10.1016/0012-821X(75)90088-6).

490 Steiner, M., Li, G., Qian, Y., Zhu, M. & Erdtmann, B.-D. 2007. Neoproterozoic to  
491 Early Cambrian small shelly fossil assemblages and a revised biostratigraphic  
492 correlation of the Yangtze Platform (China). *Palaeogeography Palaeoclimatology*  
493 *Palaeoecology*, 254, 67-99, <https://doi.org/10.1016/j.palaeo.2007.03.046>.

494 Wiedenbeck, M., Alle, P., Corfu, F., Griffin, W. L., Meier, M., Oberli, F., Vonquadt, A.,  
495 Roddick, J. C. & Spiegel, W. 1995. Three natural zircon standards for U-Th-Pb,  
496 Lu-Hf, trace element and REE analyses. *Geostandards Newsletter*, 19, 1-23,  
497 <https://doi.org/10.1111/j.1751-908X.1995.tb00147.x>.

498 Wills, M. A., Briggs, D. E. & Fortey, R. A. 1994. Disparity as an evolutionary index: a  
499 comparison of Cambrian and Recent arthropods. *Paleobiology*, 20(2), 93-130,  
500 <https://doi.org/10.1017/S009483730001263X>.

501 Yang, A., Zhu, M., Zhuravlev, A. Y., Yuan, K., Zhang, J. & Chen, Y. 2016b.  
502 Archaeocyathan zonation of the Yangtze Platform: Implications for regional and  
503 global correlation of lower Cambrian stages. *Geological Magazine*, 153(3),  
504 388-409, <https://doi.org/10.1017/S0016756815000333>.

505 Yang, B., Steiner, M., Li, G. & Keupp, H. 2014. Terreneuvian small shelly faunas of  
506 East Yunnan (South China) and their biostratigraphic implications.

507 Palaeogeography, Palaeoclimatology, Palaeoecology, 398, 28-58,  
508 <http://dx.doi.org/10.1016/j.palaeo.2013.07.003>.

509 Yang, B., Steiner, M., Zhu, M. Y., Li, G. X., Liu, J. N. & Liu, P. J. 2016a. Transitional  
510 Ediacaran-Cambrian small skeletal fossil assemblages from South China and  
511 Kazakhstan: Implications for chronostratigraphy and metazoan evolution.  
512 *Precambrian Research*, 285, 202-215,  
513 <http://dx.doi.org/10.1016/j.precamres.2016.09.016>.

514 Yang, C., Li, X. H., Zhu, M. Y. & Condon, D. J. 2017a. SIMS U-Pb zircon  
515 geochronological constraints on the stratigraphic correlations of the upper  
516 Ediacaran in South China. *Geological Magazine*, 154(6),  
517 <https://doi.org/10.1017/S0016756816001102>.

518 Yang, C., Zhu, M. Y., Condon, D. J. & Li, X. H. 2017b. Geochronological constraints  
519 on stratigraphic correlation and oceanic oxygenation in Ediacaran-Cambrian  
520 transition in South China. *Journal of Asian Earth Sciences* 140, 75-81,  
521 <http://dx.doi.org/10.1016/j.jseaes.2017.03.017>.

522 Zhang, X. L. & Shu, D. G. 2014. Causes and consequences of the Cambrian explosion.  
523 *Science China: Earth Sciences* 57(5), 930-942,  
524 <http://dx.doi.org/10.1007/s11430-013-4751-x>.

525 Zhang, X. L., Ahlberg, P., Babcock, L. E., Choi, D. K., Geyer, G., Gozalo, R.,  
526 Hollingsworth, J. S., Li, G. X., Naimark, E. B., Pegel, T., Steiner, M., Wotte, T. &  
527 Zhang, Z. F. 2017. Challenges in defining the base of Cambrian Series 2 and Stage  
528 3. *Earth-Science Reviews*, 172, 124-139,  
529 <http://dx.doi.org/10.1016/j.earscirev.2017.07.017>.

530 Zhao, F. C., Zhu, M. Y. & Hu, S.X. 2010. Community structure and composition of  
531 the Cambrian Chengjiang biota. *Science China Earth Sciences*, 53(12), 1784-1799,  
532 <http://dx.doi.org/10.1007/s11430-010-4087-8>.

533 Zhao, F. C., Hu, S. X., Caron, J. B., Zhu, M. Y., Yin, Z. J. & Lu, M. 2012. Spatial  
534 variation in the diversity and composition of the Lower Cambrian (Series 2, Stage  
535 3) Chengjiang biota, Southwest China. *Palaeogeography, Palaeoclimatology,*  
536 *Palaeoecology*, 346-347, 54-65, <http://dx.doi.org/10.1016/j.palaeo.2012.05.021>.

537 Zhu, M. Y., Li, G. X., Zhang, J. M., Steiner, M., Qian, Y. & Jiang, Z. W. 2001. Early  
538 Cambrian stratigraphy of east Yunnan, southwestern China: a synthesis. *Acta*  
539 *Palaeontologica Sinica*, 40(Sup.), 4-39.

540 Zhu, M. Y., Babcock, L. E. & Peng, S. C. 2006. *Advances in Cambrian Stratigraphy*

541 and paleontology: Integrating correlation techniques, palaeobiology, taphonomy  
542 and paleoenvironmental reconstruction. *Palaeoworld*, 15, 217-222,  
543 <http://dx.doi.org/10.1016/j.palwor.2006.10.016>.

544 Zhu, M. Y. 2010. The origin and Cambrian explosion of animals: fossil evidences  
545 from China. *Acta Palaeontologica Sinica*, 49(3), 269-287 (in Chinese with English  
546 abstract).

547 Zhu, M. Y., Zhuravlev, A. Y., Wood, R. A., Zhao, F. & Sukhov, S. S. 2017. A deep root  
548 for the Cambrian explosion: Implications of new bio-and chemostratigraphy from  
549 the Siberian Platform. *Geology*, 45(5), 459-462,  
550 <http://dx.doi.org/10.1130/G38865.1>.

551 Zhu, R. X., Li, X. H., Hou, X. G., Pan, Y. X., Wang, F., Deng, C. L. & He, H. Y. 2009.  
552 SIMS U-Pb zircon age of a tuff layer in the Meishucun section, Yunnan, southwest  
553 China: Constraint on the age of the Precambrian-Cambrian boundary. *Science in  
554 China Series D: Earth Sciences*, 52(9), 1385-1392,  
555 <http://dx.doi.org/10.1007/s11430-009-0152-6>.

556

### 557 **Figure captions**

558 Figure 1. Generalized stratigraphic column of the Xiaolantian section, Chengjiang  
559 County, eastern Yunnan, South China. The biostratigraphy is based on [Steiner \*et al.\* \(2007\)](#)  
560 [and Yang \*et al.\* \(2016a\)](#), and radiometric ages come from [Compston \*et al.\* \(2008\)](#),  
561 [Zhu \*et al.\* \(2009\)](#), and [Yang \*et al.\* \(2017a\)](#). Ashes beds are marked in red  
562 lines.

563 Figure 2. Photomicrographs of siltstone sample 14CJ-2 (a) and mudstone sample  
564 14CJ-3 (b).

565 Figure 3. CL images of zircons analysed by CA-ID-TIMS U-Pb technique. The  
566 ellipses indicate the SIMS U-Pb analytical spots with 30 microns in length for  
567 scale. SIMS zircon  $^{238}\text{U}$ - $^{206}\text{Pb}$  dates are presented in black color and CA-ID-TIMS  
568 in red. All the zircon  $^{238}\text{U}$ - $^{206}\text{Pb}$  dates are quoted with  $2\sigma$  uncertainty. Percentages  
569 in the parentheses represent the discordances defined by the SIMS  $^{238}\text{U}$ - $^{206}\text{Pb}$  and

570  $^{207}\text{Pb}$ - $^{206}\text{Pb}$  dates.

571 Figure 4. Age distribution patterns of detrital zircons from sample 14CJ-2 and 14CJ-3.

572  $^{207}\text{Pb}$ - $^{206}\text{Pb}$  ages are used for zircons older than 1000 Ma and  $^{238}\text{U}$ - $^{206}\text{Pb}$  ages for  
573 zircons younger than 1000 Ma. Only concordant or nearly concordant (<10%  
574 discordant) data are included.

575 Figure 5.  $^{238}\text{U}$ - $^{206}\text{Pb}$  results of the youngest detrital zircons analysed by SIMS and

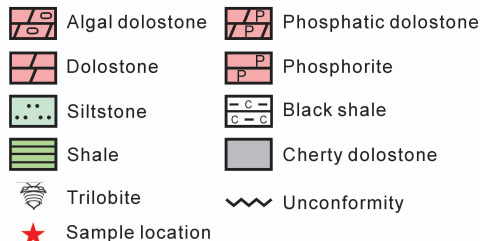
576 CA-ID-TIMS. Zircon  $^{238}\text{U}$ - $^{206}\text{Pb}$  dates are quoted with  $2\sigma$  uncertainty in (b).

577 Figure 6. Cumulative phyla and classes through the late Ediacaran - early Cambrian

578 Period in South China. Diversity data come from [Zhang & Shu \(2014\)](#), and

579 radiometric (or estimated) ages are from [Cohen \*et al.\* \(2013\)](#), [Yang \*et al.\* \(2017a\)](#),

580 and this study.



MTS: Maotianshan

ZYC: Zhongyicun

BS: Black Shale

DLT: Donglongtan

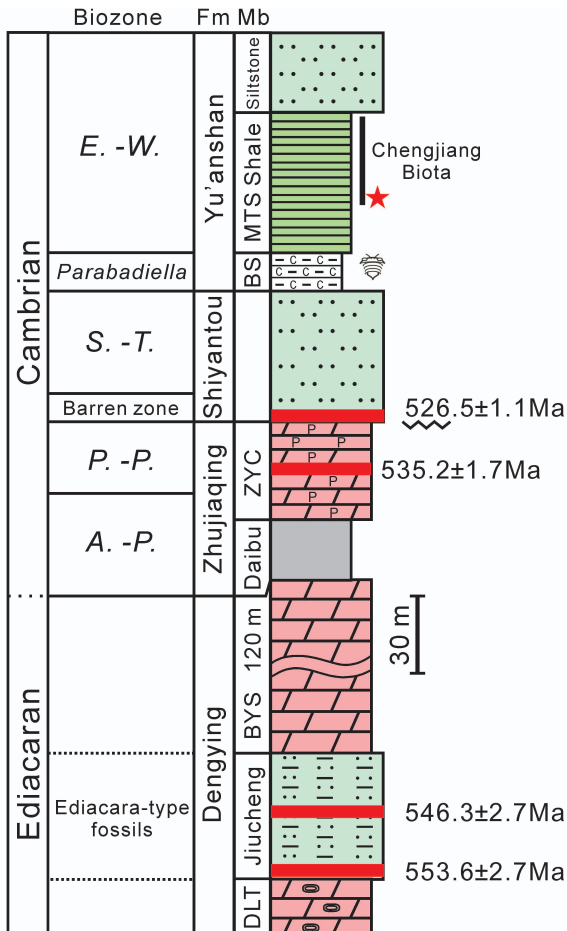
BYS: Baiyanshao

*E. -W.*: *Eoredlichia-Wutingaspis*

*S. -T.*: *Sinosachites flabelliformis-Tannuolina Zhangwentangi*

*P. -P.*: *Paragloborilus subglobosus-Purella squamulosa*

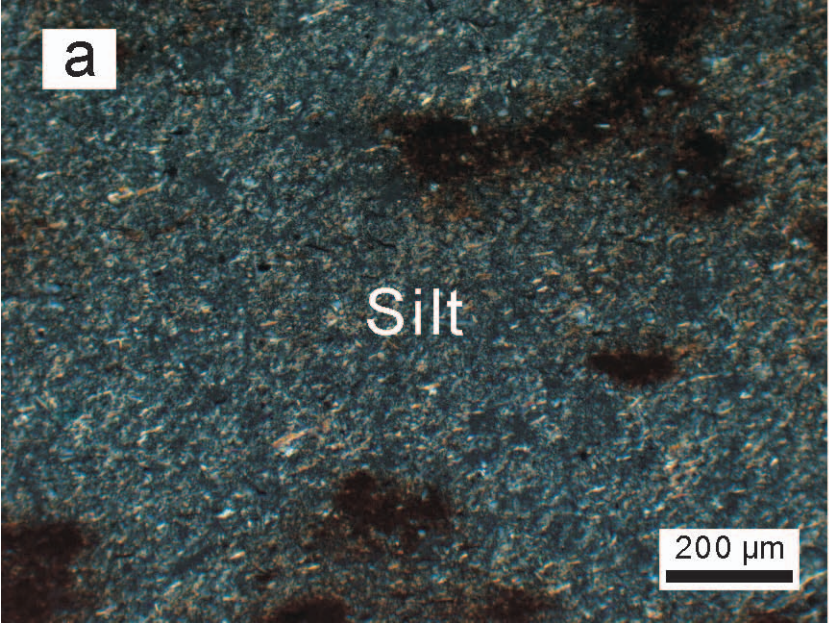
*A. -P.*: *Anabarites trisulcatus-Protohertzina anabarica*



a

Silt

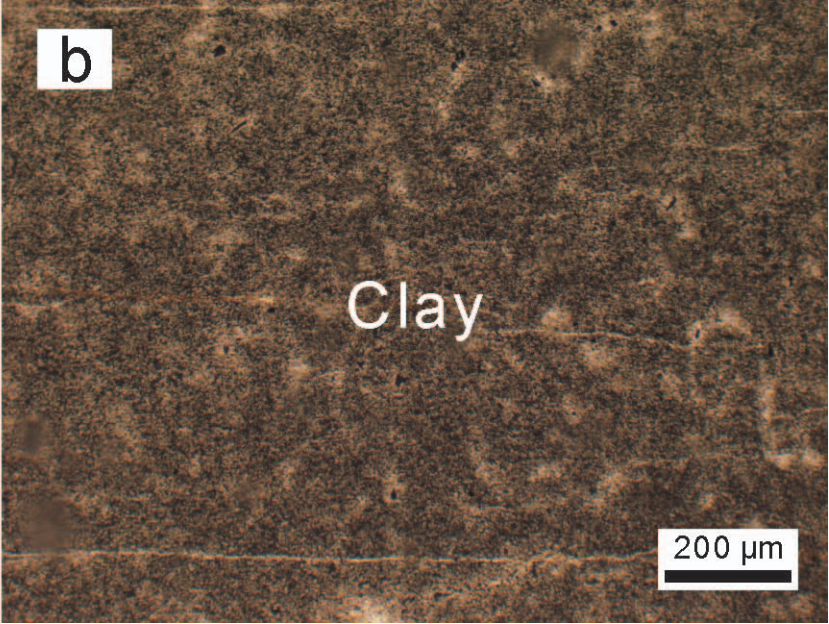
200  $\mu\text{m}$

Micrograph showing a dense, granular texture of silt soil. The particles are small and irregular, with a blueish-grey color. There are some darker, irregular patches scattered throughout the field of view. A scale bar is located in the bottom right corner.

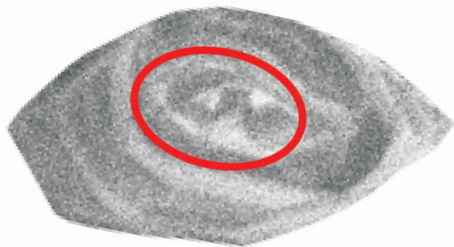
b

Clay

200  $\mu\text{m}$

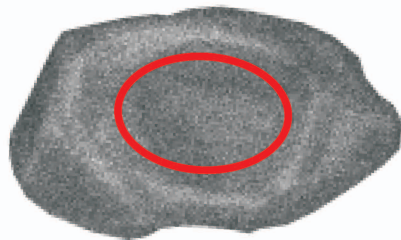
Micrograph showing a dense, granular texture of clay soil. The particles are very fine and uniform, with a brownish-grey color. There are some darker, irregular patches scattered throughout the field of view. A scale bar is located in the bottom right corner.

14CJ-2@02



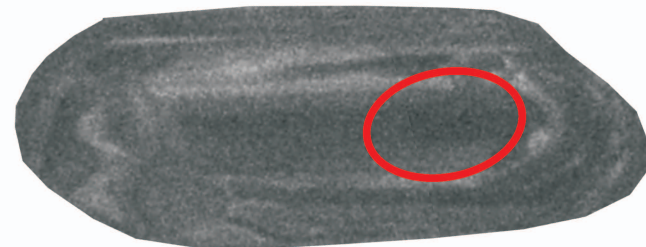
$517.5 \pm 15.0$  Ma (1.1%)  
 $524.33 \pm 0.86/0.87$  Ma

14CJ-2@29



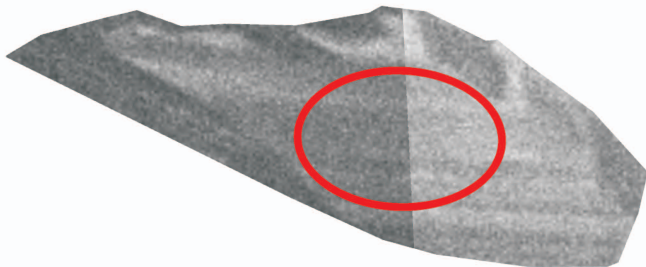
$527.8 \pm 15.2$  Ma (-0.5%)  
 $527.79 \pm 2.50/2.51$  Ma

14CJ-2@66



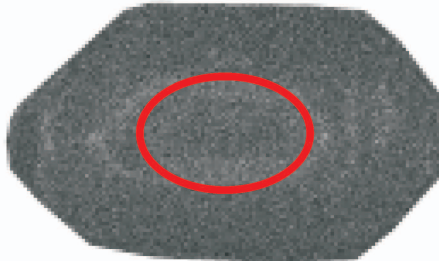
$491.9 \pm 14.4$  Ma (6.1%)  
 $584.42 \pm 1.23/1.24$  Ma

14CJ-3@07



$517.9 \pm 15.2$  Ma (1.6%)  
 $518.03 \pm 0.69/0.71$  Ma

14CJ-3@37



$499.0 \pm 14.4$  Ma (7.5%)  
Pbc = 24.9 pg

LM-23-12@45



$531.1 \pm 15.4$  Ma (0.4%)  
 $544.41 \pm 4.21/4.21$  Ma

